*Supporting Information*

# *In-situ* prepared "polymer-in-salt" electrolytes enabling high-voltage lithium metal battery

Mengjun Sun [a,b], Ziqi Zeng [a,*], Wei Zhong [a,b], Zhilong Han [a,c], Linfeng Peng [a,c], Chuang Yu [a], Shijie Cheng [a], Jia Xie [a,*]

[a] *State Key Laboratory of Advanced Electromagnetic Engineering and Technology, School of Electrical and Electronic Engineering, Huazhong University of Science and Technology, Wuhan 430074, China*

[b] *State Key Laboratory of Materials Processing and Die & Mould Technology, School of Materials Science and Engineering, Huazhong University of Science and Technology, Wuhan 430074, China*

[c] *School of Physics, Huazhong University of Science and Technology, Wuhan 430074, China*

[*] Corresponding authors.

*E-mail address*: xiejia@hust.edu.cn (J. Xie), ziqizeng@hust.edu.cn (Z. Zeng).

## 2.1 Materials

$\varepsilon$-Caprolactone ($\varepsilon$-CL, 99%), DL-Lactide (LA, 98%), stannous octoate (Sn $(Oct)_2$, 95%) and were purchased from Aladdin. Lithium bis(trifluoromethanesulphonyl)imide (LiTFSI, 99%) and lithium difluoro oxalate borate (LiDFOB) were purchased from Capchem and Do-Fluoride New Materials Co., Ltd.. A number of activated molecular sieve were used to remove the trace amounts of water of $\varepsilon$-CL and Sn $(Oct)_2$. Polyethylene separator about 8 μm was provided by Changzhou Senior New Energy Materials Co., Ltd. and the detailed information of the separator are shown in Table S4.

## 2.3 Materials characterization

A Fourier-transform infrared spectra FTIR test was conducted on a Bruker Vertex 70 spectrometer (the frequency range is 400 – 4000 $cm^{-1}$). The $^1H$ nuclear magnetic resonance (NMR) spectrum were obtained using a Bruker 400 MHz spectrometer. CL, LA and the obtained PEs were dissolved in $CDCl_3$ for $^1H$ NMR testing. All samples were prepared in glove box. The morphologies of Li foil were investigated by a scanning electron microscope (SEM, Nova NanoSEM 450, FEI). X-ray photoelectron spectroscopy (XPS) was performed using an AXIS-ULTRA DLD-600W (Shimadzu-Kratos Co., Ltd.). Alternating-current impedances (AC) impedances, cyclic voltammetry (CV) and linear sweep voltammetry (LSV) tests are implemented by CHI660E electrochemical workstation *(Chenhua, Shanghai, China).*

## Supplementary Figures:

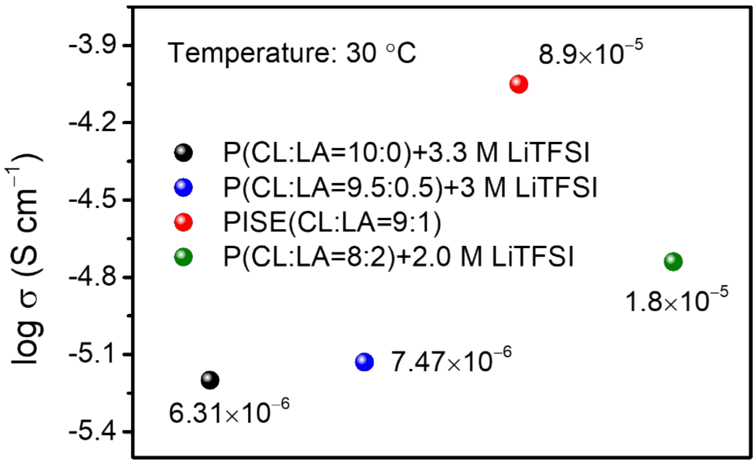


**Fig. S1** The ionic conductivity of PCL-based electrolytes with different mass ratio of CL and LA.

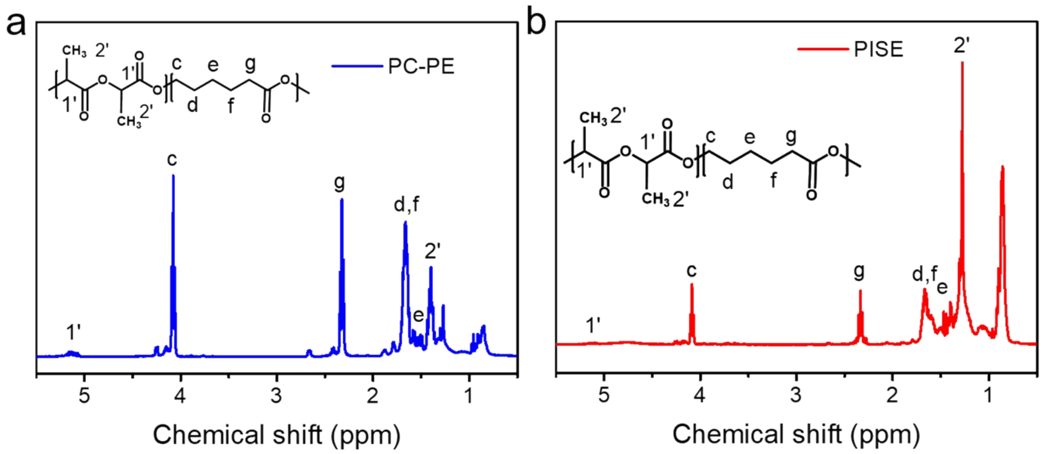


**Fig. S2** Characterization of the *in-situ* PISE. $^1$H NMR spectra of (a) PCA-PE and (b) PISE.

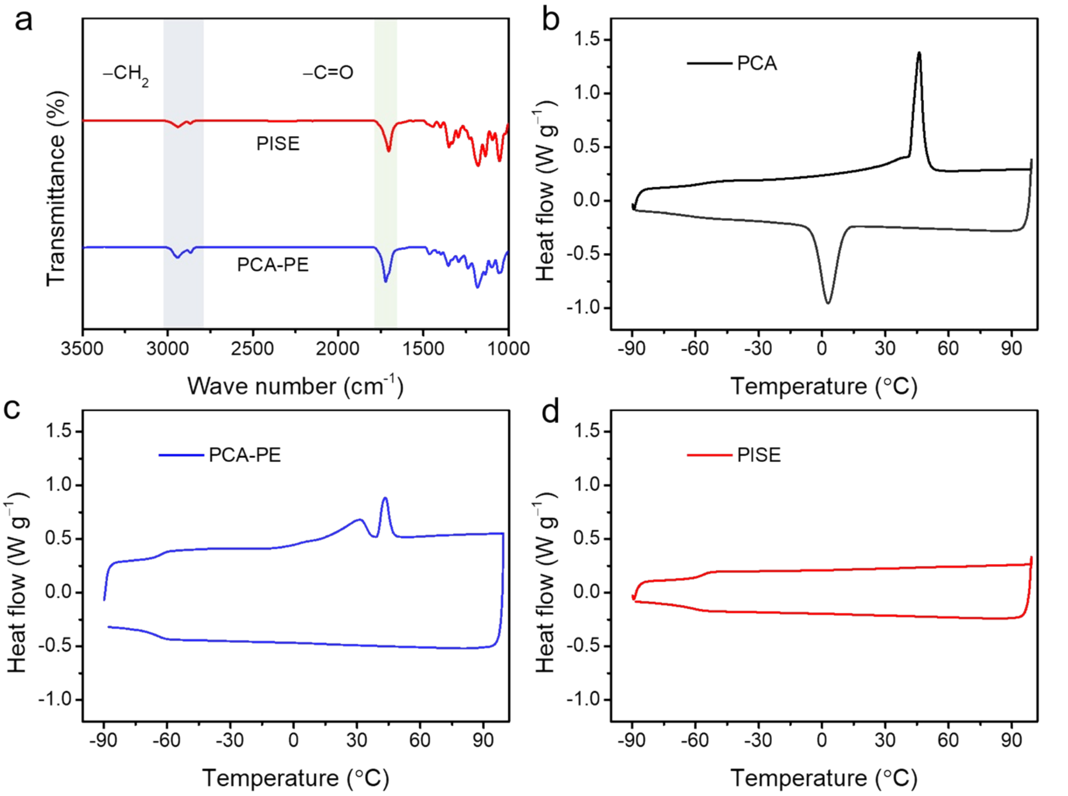


**Fig. S3 (a)** FTIR spectrum comparison of PCA-PE and PISE. (b-d) DSC profiles of PCA and PEs.

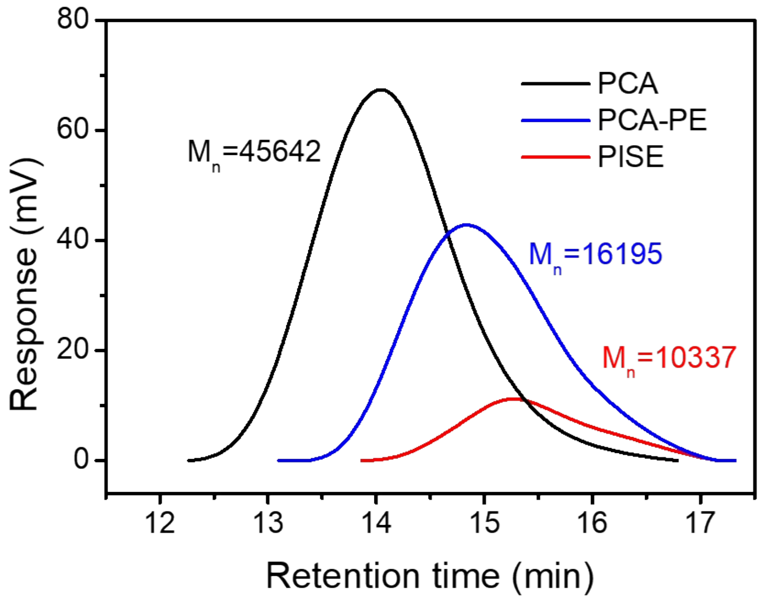


**Fig. S4** Gel permeation chromatography (GPC) of PCA, PCA-PE and PISE.

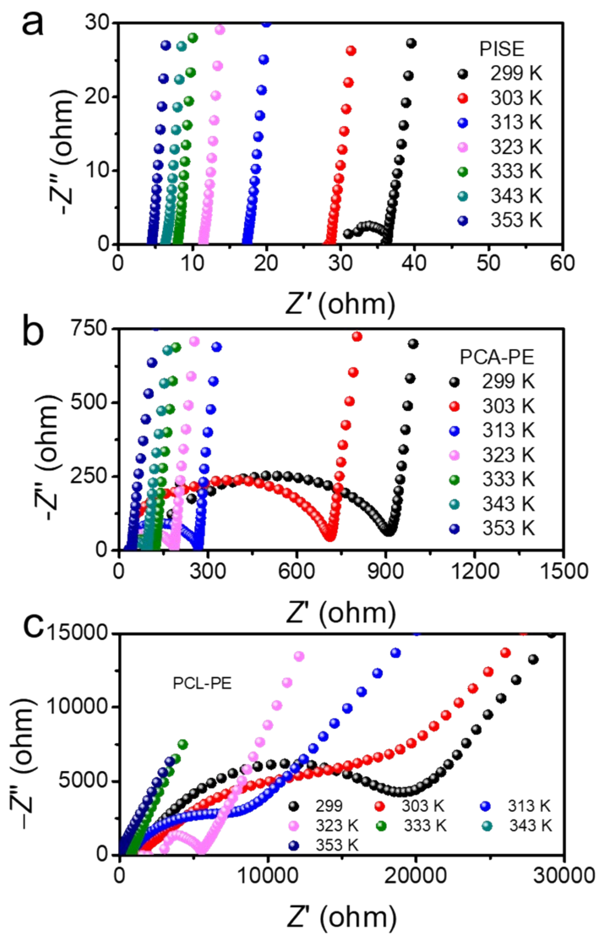


**Fig. S5** Electrochemical characteristics of *in-situ* PCLA-based electrolytes. EIS curves of (a) SS/*in-situ* PCLA-PE1/SS, (b) SS/*in-situ* PISE/SS symmetric cell at different temperature.

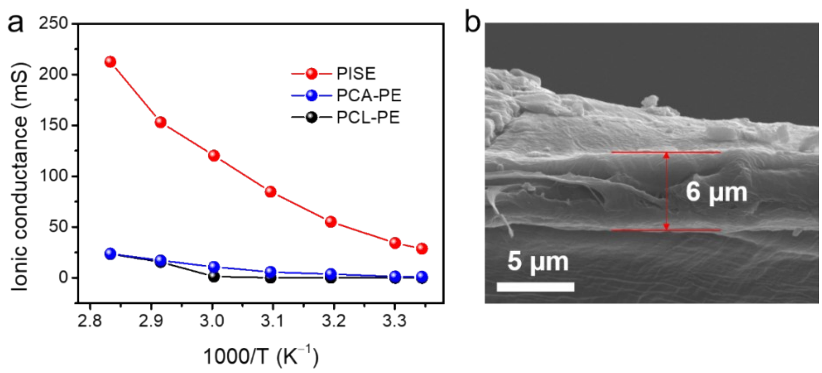


**Fig. S6** (a) The temperature-dependent ionic conductance of PISE. (b) Cross-section SEM images of the PE separator after *in-situ* polymerization of *ε*-CL and LA.

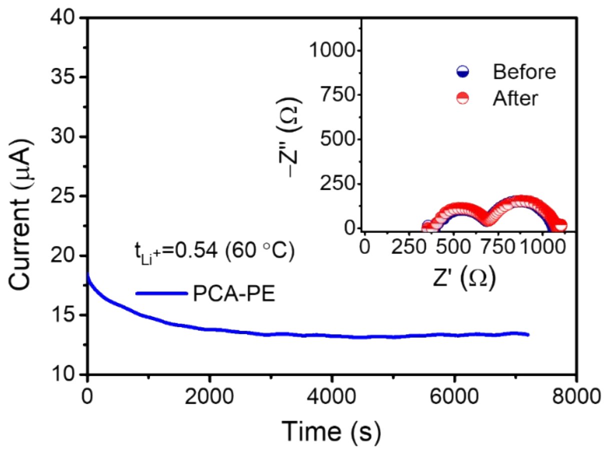


**Fig. S7** Chronoamperometry profile under a potential of 10 mV and the EIS spectra before and after the polarization test.

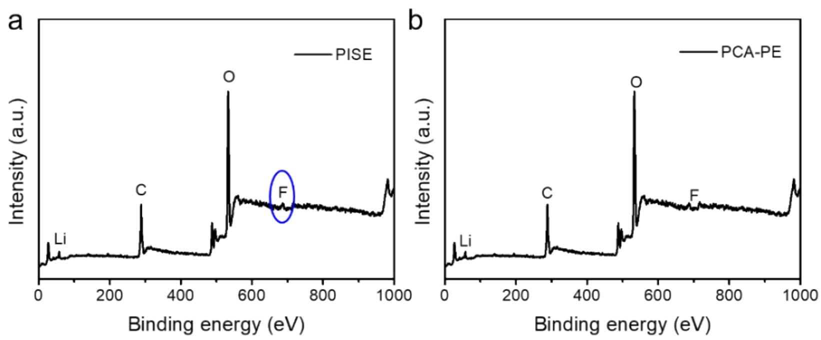


**Fig. S8** XPS spectra of lithium surface of the cycled Li/Li symmetrical battery with *in-situ* (a) PISE and (b) PCA-PE.

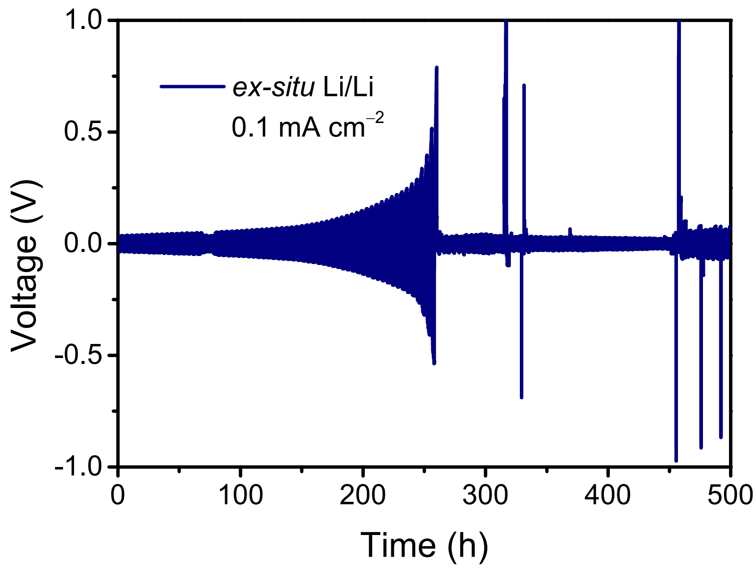


**Fig. S9** Cycling stability of *ex-situ* Li/Li symmetrical cells based on PISE at 30 °C.

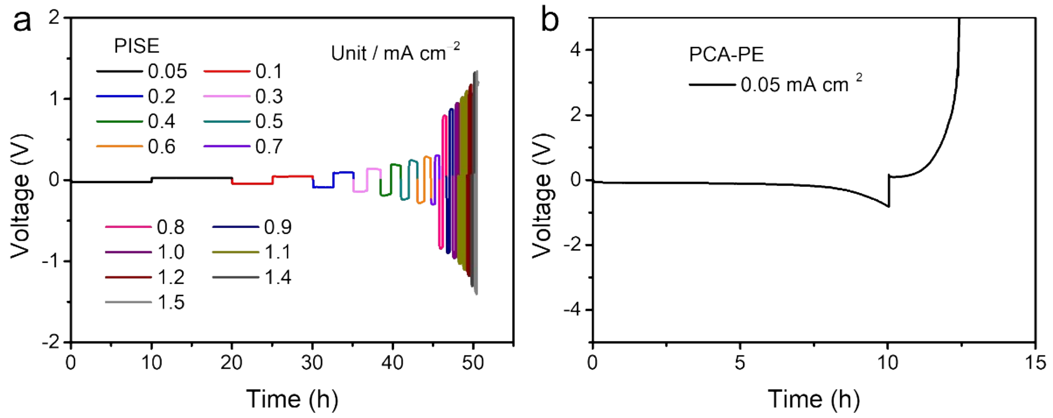


**Fig. S10** Li plating/stripping overpotential profiles in the (a) Li/PISE/Li cell and (b) Li/PCA-PE/Li cell at step-increased current densities.

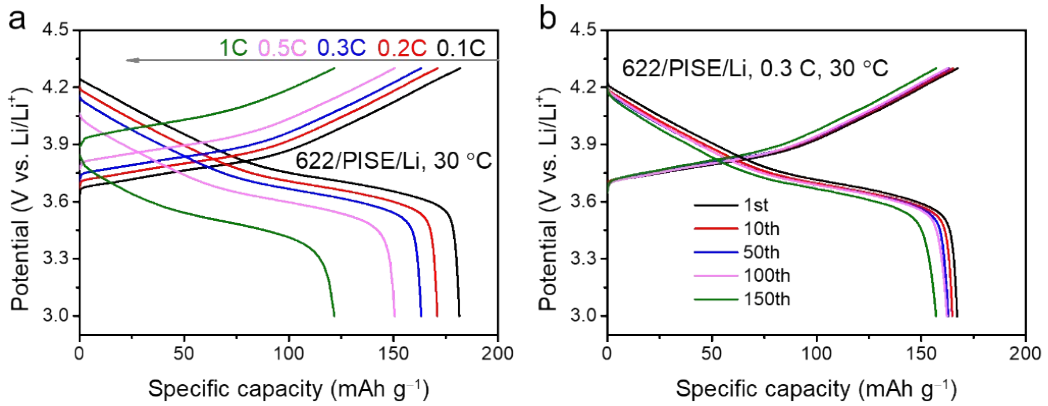


**Fig. S11** (a) Charge/discharge profiles for *in-situ* NCM622/PISE/Li cells at different current density. (b) Galvanostatic charge/discharge profiles for *in-situ* NCM622/PISE/Li cells at 0.3 C.

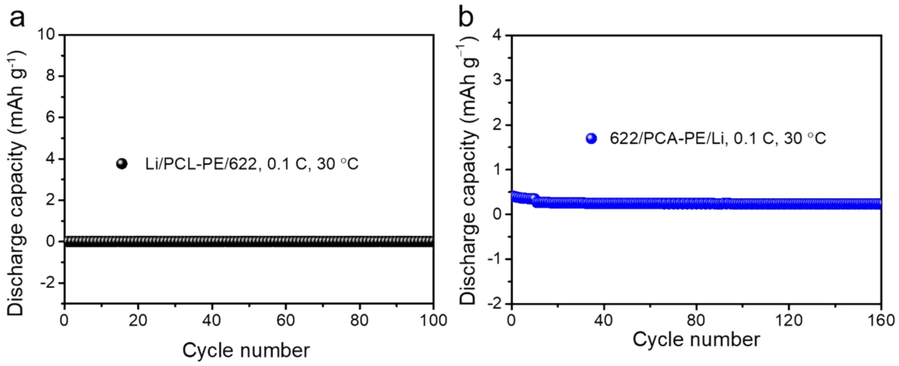


**Fig. S12** Cycling performances of the NCM622/Li cells based on PCA-PE with the voltage range of 3.0−4.3 V.

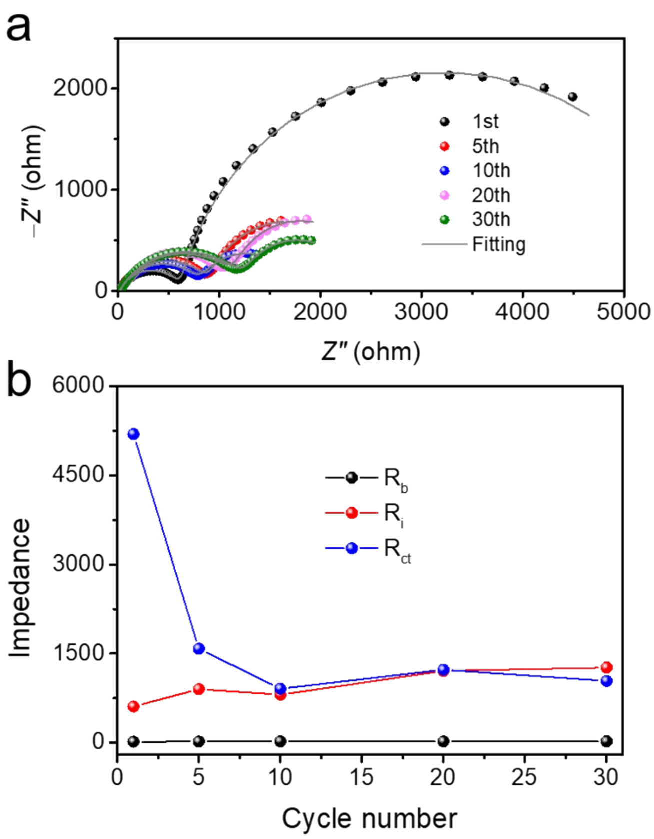


**Fig. S13** Resistances of NCM811/*in-situ* PISE/Li cell after cycling at 30 ℃.

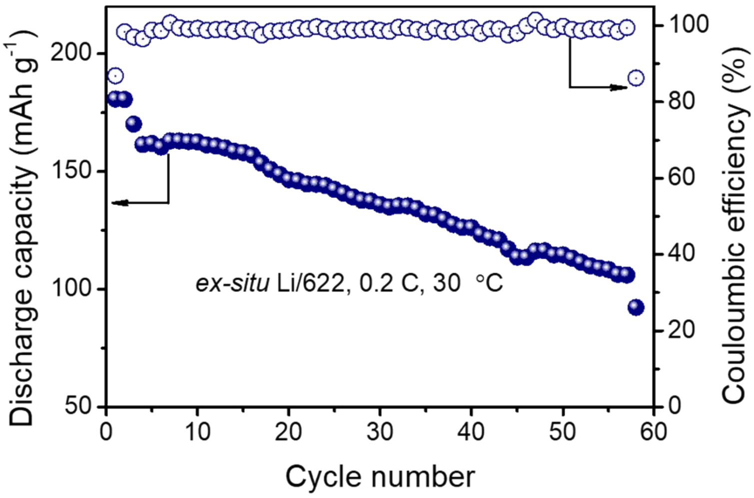


**Fig. S14** Cycling performances of the NCM622/*ex-situ* PISE/Li cells at 0.2 C in the voltage range of 3.0−4.3 V.

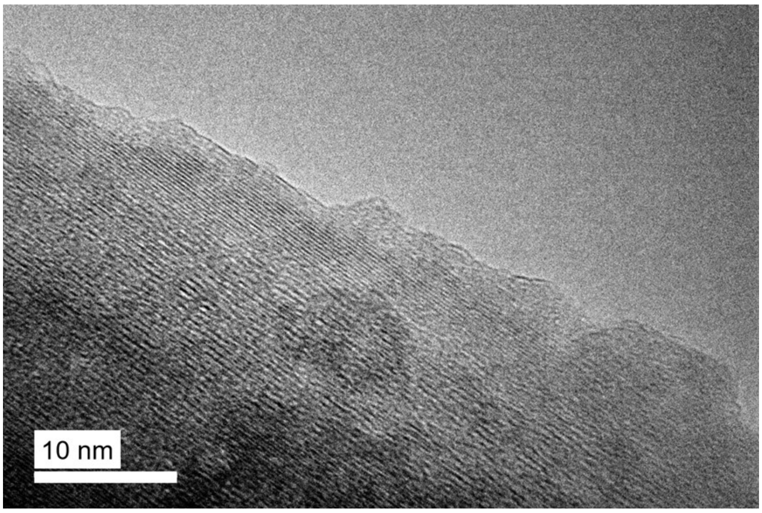


**Fig. S15** TEM images of NCM622 after cycling test in PISE.

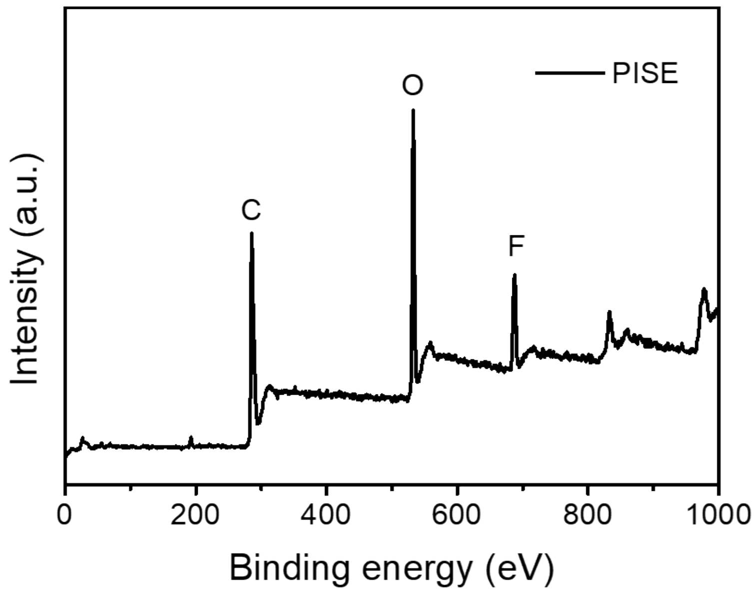


**Fig. S16** XPS spectra of lithium surface of the cycled NCM622/Li battery with *in-situ* PISE.

## Supplementary Tables

**Table S1** Composition of the different polymer electrolytes

| | **Concentration of LiTFSI (mol L$^{-1}$)** | **Concentration of LiDFOB (mol L$^{-1}$)** | **Mass ratio of Sn (Oct)$_2$** |
|---|---|---|---|
| **PCL** | 0 | 0 | 10 wt% |
| **PCA** | 0 | 0 | |
| **PCL-PE** | 1 | 0.3 | |
| **PCA-PE** | 1 | 0.3 | |
| **PISE** | 3.0 | 0.3 | |

**Table S2** The solubility of LiTFSI in the solution with different mass ratio of CL and LA.

| $\frac{m_{CL}}{m_{LA}}$ | | 10:0 | 9.5:0.5 | 9:1 | 8:2 | 7.5:2.5 |
|---|---|---|---|---|---|---|
| Lithim concentration | 1 M LiTFSI | 🏱 | 🏱 | 🏱 | 🏱 | 🏳 |
| | 2 M LiTFSI | 🏱 | 🏱 | 🏱 | 🏱 | 🏳 |
| | 3 M LiTFSI | 🏱 | 🏱 | 🏱 (PISE) | 🏳 | 🏳 |
| | 3.3 M LiTFSI | 🏱 | 🏳 | 🏳 | 🏳 | 🏳 |

**Table S3** Melting enthalpy, crystallinity and melting point of the different polymer electrolytes.

| Composition | $\Delta H_m$ (J/g) | Crystallinity (%) | $T_m$ (°C) | $T_g$ (°C) |
|---|---|---|---|---|
| **PCA** | 33.4 | 24.9 | 45.8 | −60 (Ref. 1) |
| **PCA-PE** | 4.53 | 3.4 | 40.6 | −62 |
| **PISE** | Amorphous | | | −72.2 |

**Table S4** GPC test results of PEVC-PE with different concentration of lithium salt.

| | $M_n$ | $M_w$ | PDI |
|---|---|---|---|
| **PCA** | 45642 | 84591 | 1.85 |
| **PCA-PE** | 29223 | 58244 | 1.99 |
| **PISE** | 10337 | 17022 | 1.64 |

**Table S5** The detailed information of the separator.

| **Product type** | **SW507E** | |
|---|---|---|
| **Items** | **unit** | **Test data** |
| Thickness | μm | 7.4 |
| Basis weight | $g/m^2$ | 4.1 |
| Permeability | s/100 mL | 115 |
| Porosity | % | 42.3 |
| Puncture strength | gf | 376.9 |
| Tensile strength/MD | $Kgf/cm^2$ | 2443 |
| Tensile strength/TD | | 2575 |
| Heat shrinkage/MD (120 °C/1 h) | % | 5.0 |
| Heat shrinkage/TD (120 °C/1 h) | % | 4.9 |

## Reference

[1] B. Zhang, Y. Liu, J. Liu, L. Liu, L. Sun, L. Cong, F. Fu, A. Mauger, C.M. Julien, H. Xie, X. Pan, "Polymer-in-ceramic" based poly($\varepsilon$-caprolactone)/ceramic composite electrolyte for all-solid-state batteries, J. Energy Chem. 2021， 52， 318. https://doi.org/10.1016/j.jechem.2020.04.025.